

# Wnt-Ryk signalling mediates medial-lateral retinotectal topographic mapping

Adam M. Schmitt<sup>1\*</sup>, Jun Shi<sup>1\*</sup>, Alex M. Wolf<sup>2</sup>, Chin-Chun Lu<sup>1</sup>, Leslie A. King<sup>2</sup> & Yimin Zou<sup>1,2,3</sup>

**Computational modelling has suggested that at least two counteracting forces are required for establishing topographic maps. Ephrin-family proteins are required for both anterior-posterior and medial-lateral topographic mapping, but the opposing forces have not been well characterized. Wnt-family proteins are recently discovered axon guidance cues. We find that *Wnt3* is expressed in a medial-lateral decreasing gradient in chick optic tectum and mouse superior colliculus. Retinal ganglion cell (RGC) axons from different dorsal-ventral positions showed graded and biphasic response to *Wnt3* in a concentration-dependent manner. *Wnt3* repulsion is mediated by Ryk, expressed in a ventral-to-dorsal decreasing gradient, whereas attraction of dorsal axons at lower *Wnt3* concentrations is mediated by Frizzled(s). Overexpression of *Wnt3* in the lateral tectum repelled the termination zones of dorsal RGC axons *in vivo*. Expression of a dominant-negative Ryk in dorsal RGC axons caused a medial shift of the termination zones, promoting medially directed interstitial branches and eliminating laterally directed branches. Therefore, a classical morphogen, *Wnt3*, acting as an axon guidance molecule, plays a role in retinotectal mapping along the medial-lateral axis, counterbalancing the medial-directed EphrinB1-EphB activity.**

Topographic mapping of axonal connections is a fundamental and widespread feature of nervous system wiring, whereby spatial orders of neurons are smoothly and continuously mapped to their targets. Molecular labels in the target fields specify topographic connections by activating receptors expressed in growth cones. Classical studies and computational modelling propose that balanced opposing forces are necessary for generating smooth topographic maps<sup>1–4</sup>. The ephrin family of proteins have been identified as axon guidance cues important for map formation.

The retinotectal projections are organized along the anterior-posterior and dorsal-ventral axes. Temporal axons terminate at anterior tectum, and nasal axons project to the posterior tectum. Ventral retinal axons connect to medial (dorsal) tectum, and dorsal retinal axons find their targets at lateral (ventral) tectum. Studies implicated A-class ephrins in establishing anterior-posterior topographic mapping via a repulsive mechanism through the EphA receptors<sup>5–8</sup>. Along the medial-lateral axis, an attractive interaction involving EphrinB-EphB was proposed to control dorsal-ventral patterning<sup>9,10</sup>.

Our previous work identified Wnts as guidance molecules for ascending spinal cord commissural axons<sup>11</sup> and descending cortico-spinal tract axons<sup>16</sup>. Here we report evidence that a classical morphogen, *Wnt3*, acts as an axon guidance molecule and plays an essential role in medial-lateral topographic map formation by counterbalancing the opposing medial-directed cue, EphrinB1<sup>10</sup>. The identification of *Wnt3* as a counterbalancing cue to EphrinB1 provides the first direct experimental evidence for theoretical models of counterbalancing forces in topographic neural map formation<sup>1,2</sup>.

## **Wnt3 is expressed in a medial-lateral decreasing gradient**

*In situ* hybridization showed that *Wnt3* is expressed in a high-to-low gradient along the medial (dorsal)-to-lateral (ventral) axis in the ventricular zone in chick optic tectum at embryonic day 10 (E10) (Fig. 1a) and mouse superior colliculus at postnatal day 0 (P0)

(Fig. 1b), similar to the expression pattern of EphrinB1 (Fig. 1c). At these stages, RGC axons have just arrived at the anterior end of the optic tectum and superior colliculus and have begun to be patterned on the pial surface. Sense controls are in Supplementary Fig. 1a and b. The *in situ* hybridization results were quantified by measuring the signal intensity using NIH Image J (Fig. 1d–f).

Both ephrinAs and ephrinB1 transcripts are found in the ventricular zone and their proteins are thought to be transported along radial glial cells to the pial surface of the superior colliculus<sup>10,12</sup>. To test whether *Wnt3* protein is also transported to the pial surface, we performed western blotting using an anti-*Wnt3* antibody (Zymed Laboratories, Inc). Tectal tissues were isolated from the superficial layers of chick optic tectum from different medial-lateral positions and tissue lysates were equally loaded (1.5 µg protein per well) as indicated by the α-tubulin control (Fig. 1g). *Wnt3* protein was detected with a continuous medial-to-lateral decreasing gradient (M to L in Fig. 1g).

## **Biphasic and positional-dependent responses to Wnt3**

To determine whether *Wnt3* can regulate the growth of RGC axons, we first examined their growth on polycarbonated filters coated with membrane fractions of HEK293 cells expressing *Wnt3*, taking advantage of the fact that *Wnt3* is highly hydrophobic and associates tightly with cell membranes<sup>13,14</sup>. We found that *Wnt3*-transfected HEK293 cell membranes inhibited the growth of both dorsal and ventral mouse RGC axons at higher concentrations, and stimulated the growth of dorsal but not ventral RGC axons at lower concentrations (not shown). To obtain sufficient and consistent amounts of *Wnt3*, we overexpressed mouse *Wnt3* in SF9 cells using the Baculovirus system and tested the effects of different concentrations of affinity-purified *Wnt3* protein (coated with 0 ng ml<sup>-1</sup>, 0.8 ng ml<sup>-1</sup>, 4 ng ml<sup>-1</sup> and 20 ng ml<sup>-1</sup>) on chick RGC axons from six different dorsal-ventral positions (1–6 in Supplementary Fig. 2a). We found that at lower *Wnt3* concentrations, the growth of dorsal RGC axons

<sup>1</sup>Department of Neurobiology, Pharmacology and Physiology, Committees on <sup>2</sup>Developmental Biology and <sup>3</sup>Neurobiology, University of Chicago, Chicago, Illinois 60637, USA.

\*These authors contributed equally to this work.

was stimulated, whereas that of ventral axons was inhibited. At higher concentrations, both dorsal and ventral axon growth were inhibited (Fig. 1h). As a control, we performed the same series of experiments using control proteins from mock infected SF9 cells and found no attractive or repulsive effects (data not shown). Repulsion does not appear to be due to toxicity of the Wnt3 protein preparation because Wnt3 repulsion can be blocked by antibodies against Ryk (see below). Quantification is shown in Supplementary Fig. 2b. We tested retinal explants from different nasal and temporal positions and found that along the nasal–temporal axis, RGC axons did not display a graded responsiveness to Wnt3, suggesting that Wnt3 does not affect anterior–posterior topographic maps (not shown). Similar experiments were also performed with mouse retinal tissues from different dorsal ventral positions in different concentrations of Wnt3, which showed similar graded responsiveness (not shown).

### Ryk is expressed in a ventral-to-dorsal decreasing gradient in RGCs

We found that Ryk, the mammalian homologue of a repulsive Wnt receptor, Derailed<sup>15</sup>, mediates repulsion of cortical axons by Wnts<sup>16</sup>. *In situ* hybridization showed that *Ryk* is expressed in a ventral-to-dorsal decreasing gradient in the RGCs of chick as early as E6

(Fig. 2a). In contrast, no dorsal–ventral gradient was observed with *frizzled5* at the same stage (Fig. 2b). At a later stage (E10 in chick), *Ryk* was also found expressed in a ventral-to-dorsal decreasing gradient in the RGC layer (Fig. 2c, d). No dorsal–ventral gradient of *frizzled5* expression was observed (Fig. 2e, f). Sense control is shown in Supplementary Fig. 1c and d. In mouse P0 retina, a similar dorsal–ventral gradient of *Ryk* mRNA was observed (Fig. 2g, h) and no dorsal–ventral gradient of *frizzled5* was detected (not shown). Because retinal tissues become much larger at E10 in chick and P0 in mouse, we showed higher magnification pictures from dorsal and ventral retina (Fig. 2c–h). Quantifications of *in situ* measurements are shown in Fig. 2i–k.

To determine the protein distribution of Ryk, we generated antibodies against the ectodomain of Ryk and performed immunohistochemistry. We first tested specificity of the Ryk antibodies by western blotting of E11.5 mouse embryonic extracts, and found that it recognized a highly specific band of the predicted size of 90 kD (Supplementary Fig. 4e)<sup>17</sup>. Immunostaining with chick E8 retina showed that Ryk protein is highly enriched on the axons of RGCs (Supplementary Fig. 3a–l). The immunoreactive signals on the RGC axon layer in ventral retina detected by Ryk antibodies (Supplementary Fig. 3a) co-localized with  $\beta$ -tubulin staining (E7 from Developmental

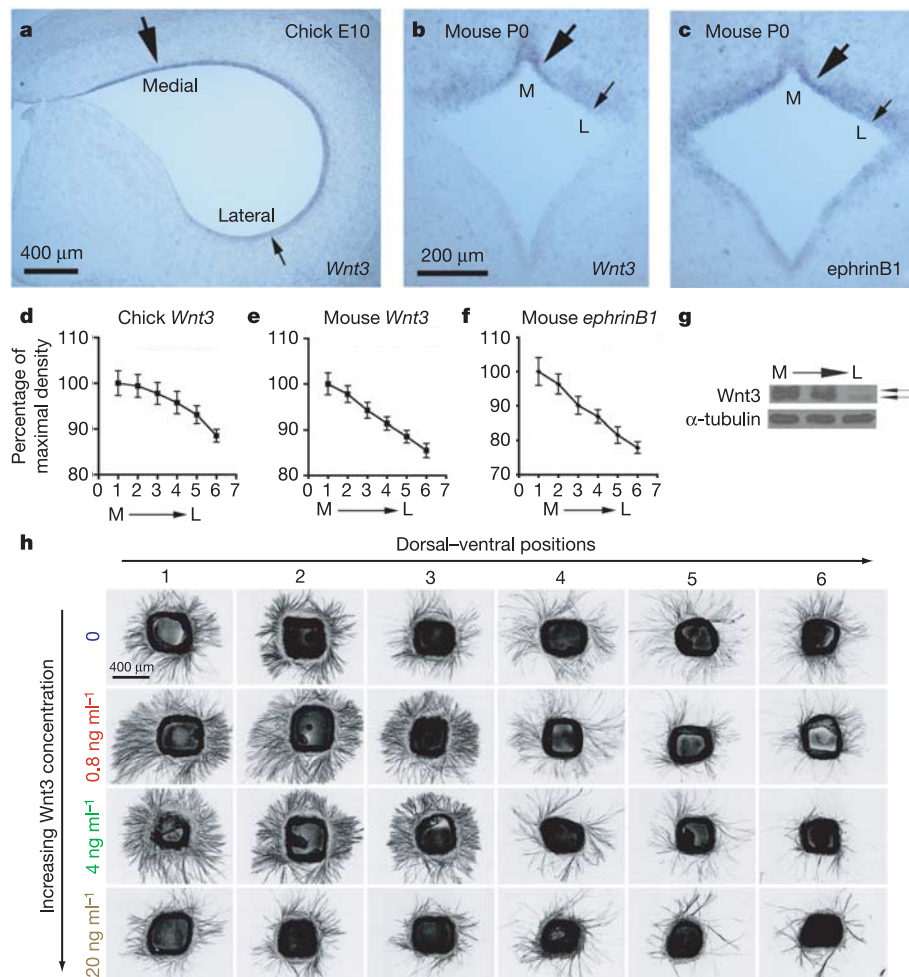


**Figure 1** | *Wnt3* expression is graded in vertebrate midbrain and *Wnt3* differentially regulated retinal axon outgrowth along the dorsal–ventral axis. **a–f**, *In situ* hybridization demonstrating expression gradients in the ventricular zone (arrows) of *Wnt3* in E10 chick tectum (**a**) and P0 mouse superior colliculus (**b**), and *ephrinB1* in P0 mouse superior colliculus (**c**), and quantification of *in situ* signal intensity (**d–f**). **g**, Western blot of membrane protein extracts from superficial optic tectum of E10 chick by anti-*Wnt3* antibodies, showing medial-to-lateral decreasing gradient with

$\alpha$ -tubulin as a loading control. Multiple bands may represent post-translational modifications. **h**, Retina explant assay. E6 chick RGC explants from six dorsal–ventral positions (diagram in Supplementary Fig. 2a) were cultured on cover slips coated with control (0 ng ml<sup>-1</sup>) and *Wnt3* protein at three concentrations (0.8 ng ml<sup>-1</sup>, 4 ng ml<sup>-1</sup> and 20 ng ml<sup>-1</sup>), with quantification of outgrowth (Supplementary Fig. 2b). Scale bars: **a**, 400  $\mu$ m; **b**, **c**, 200  $\mu$ m; **h**, 400  $\mu$ m. M, medial; L, lateral. The error bars in all figures are s.e.m.

Biology Hybridoma Bank; Supplementary Fig. 3c), as indicated by the overlapping areas (yellow) in Supplementary Fig. 3d. Very little staining in the cell body was observed at this stage (indicated by DAPI nuclear staining in Supplementary Fig. 3b). Because axons from the entire dorsal–ventral axis project radially towards the optic disc to leave the eye, it is not possible to discern a potential gradient within the axon layer. At a later stage (E10), Ryk protein continues to be enriched in axons (Supplementary Fig. 3e–l), indicated by the overlapping areas with  $\beta$ -tubulin staining (yellow) in Supplementary Fig. 3h and l. At this stage, Ryk protein can be seen in the cell bodies of RGCs. Protein levels of Ryk on the ventral RGC cell bodies were found to be much higher than on the dorsal RGC cell bodies (Supplementary Fig. 3e, i), similar to the patterns of mRNA expression (Fig. 2c, d) (arrow in Supplementary Fig. 3e indicates axon layer).

We found that Ryk is a high-affinity receptor for Wnt3 with a  $K_d$  of 4.473 nM, and the  $K_d$  for the Wnt3–Frizzled5 interaction is 39.91 nM (Supplementary Fig. 4d). Frizzled3 has similar affinity to Wnt3 as Frizzled5 (not shown). Therefore, Ryk is a higher-affinity receptor for Wnt3 than Frizzled5 and Frizzled3.

We found that anti-Ryk antibodies ( $50 \mu\text{g ml}^{-1}$ ) can specifically block Wnt3–Ryk binding (Supplementary Fig. 4g,  $P < 0.0001$ ) but not Wnt3–Frizzled5 binding (Supplementary Fig. 4j,  $P = 0.1069$ ). In contrast, sFRP2 ( $0.2 \mu\text{g ml}^{-1}$ ) can block Wnt–Frizzled5 binding (Supplementary Fig. 4i,  $P = 0.0045$ ) but cannot block Wnt–Ryk binding (Supplementary Fig. 4h,  $P = 0.1094$ ). Similar results held true for Frizzled3 (not shown). The mechanism of Wnt–Ryk binding may be different from that of Wnt–Frizzled. The Wnt-binding domain in the Frizzled protein is the cysteine rich domain (CRD)<sup>18</sup> and the domain in Ryk for Wnt binding is the structurally unrelated Wnt-inhibitory factor (WIF) domain<sup>19,20</sup>. Because of the differential blocking effect, sFRP2 protein and anti-Ryk antibodies can be used to tease apart the function of Frizzled and Ryk, by specifically blocking the binding of Wnt3 to Frizzled(s) or Ryk, respectively.

### Ryk mediates inhibition and Frizzleds mediate stimulation

We tested whether anti-Ryk antibodies can block the Wnt3 effects on dorsal and ventral axons at low and high concentrations ( $0.8 \text{ ng ml}^{-1}$  and  $20 \text{ ng ml}^{-1}$ ) (Fig. 3). For dorsal retinal explants, we dissected

and cultured the retinal tissue from position 2, as indicated in Supplementary Fig. 2a. For ventral explants, we used position 5, as shown in Supplementary Fig. 2a. We found that the inhibition of ventral axons by Wnt3 at both concentrations, and that of dorsal axons at  $20 \text{ ng ml}^{-1}$ , can be blocked by the Ryk antibodies ( $50 \mu\text{g ml}^{-1}$ ). However, Wnt3-mediated stimulation of dorsal axons at  $0.8 \text{ ng ml}^{-1}$  cannot be blocked by the anti-Ryk antibodies (Fig. 3a).

Several lines of evidence suggest that the Ryk antibodies are highly specific. The specificity of the Ryk antibodies was first tested by western blot (Supplementary Fig. 4e). In binding assays, the Ryk antibodies only blocked the binding of Wnt3 to Ryk (Supplementary Fig. 4g) but not the binding to Frizzled5, suggesting that the Ryk antibodies do not cross-react with Frizzled5 (Supplementary Fig. 4j) or Frizzled3 (not shown). In addition, the Ryk antibodies did not block the stimulation of dorsal RGC axons by low concentrations of Wnt3 (Fig. 3a). This result itself also serves as an internal control for the specificity of the antibodies. To further test the specificity of the anti-Ryk antibodies, we performed two additional control experiments, whereby we found that Ryk antibodies do not block Slit2 repulsion and Wnt4 attraction of post-crossing commissural axons (published in Fig. 4c–f in ref. 16).

Neither preimmune nor anti-Ryk postimmune sera had any effect on the growth of RGC axons in the absence of Wnt3 (blue bars in Fig. 3b, c), suggesting that the rabbit sera did not promote growth in general. It is interesting that the Ryk antibodies allowed for Wnt3-mediated growth promotion (red bars in pre-immune and anti-Ryk in Fig. 3b and c). It is possible that the growth cones of dorsal RGC axons have both attractive and repulsive signalling pathways. When repulsion is inhibited by the Ryk antibodies, the attractive pathway takes over and shifts the balance. It should be noted that although anti-Ryk antibodies completely blocked the inhibition of dorsal RGC axons at a higher Wnt3 concentration ( $20 \text{ ng ml}^{-1}$ ) (green bars in preimmune and anti-Ryk in Fig. 3b), they did not completely block Wnt3 inhibition of ventral axons, particularly at a high concentration (up to 80% for  $0.8 \text{ ng ml}^{-1}$  and up to 55% for  $20 \text{ ng ml}^{-1}$ ) (red and green bars in preimmune and anti-Ryk in Fig. 3c). This could be because the ventral axons express more Ryk or the antibodies have limited efficacy. One also cannot exclude the possibility that the

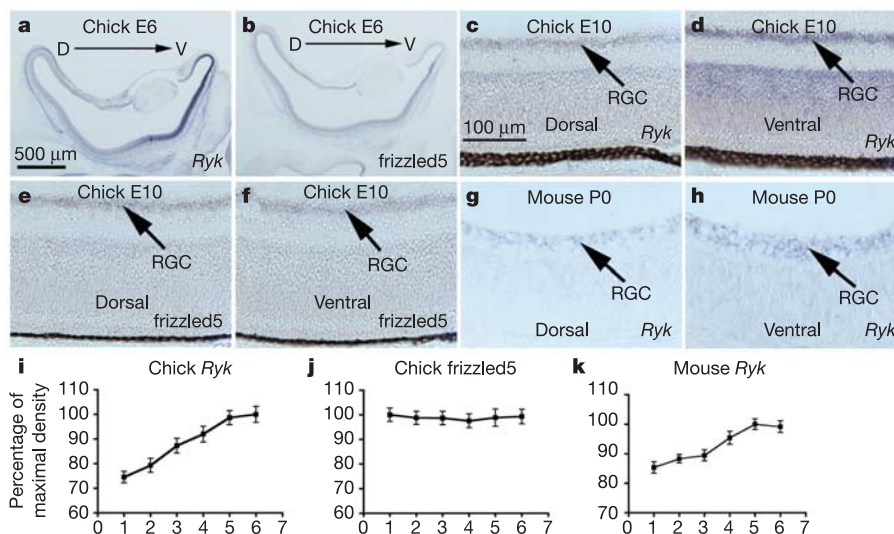


**Figure 2 | Graded expression of Ryk in chick and mouse retinal ganglion cells.** a–k, *In situ* hybridization and signal intensity quantification. Ryk mRNA is expressed in a ventral-to-dorsal decreasing gradient in E6 chick retina (a), while frizzled5 transcript is expressed evenly (b). Higher magnification of Ryk *in situ* hybridization in E10 dorsal (c) and ventral (d) chick retina and *in situ* hybridization of frizzled5 in dorsal (e) and ventral (f)

E10 chick retina. g, h, Higher magnification of Ryk *in situ* hybridization in dorsal (g) and ventral (h) P0 mouse retina. Quantification of *in situ* hybridization signal intensity along the dorsal–ventral axis of Ryk (i) and frizzled5 (j) in E10 chick retina, and Ryk expression in P0 mouse retina (k). Scale bars: a, b, 500  $\mu\text{m}$ ; c–h, 100  $\mu\text{m}$ . Numbers 1–6 represent six different positions along the dorsal–ventral axis of the retina (Supplementary Fig. 2a).

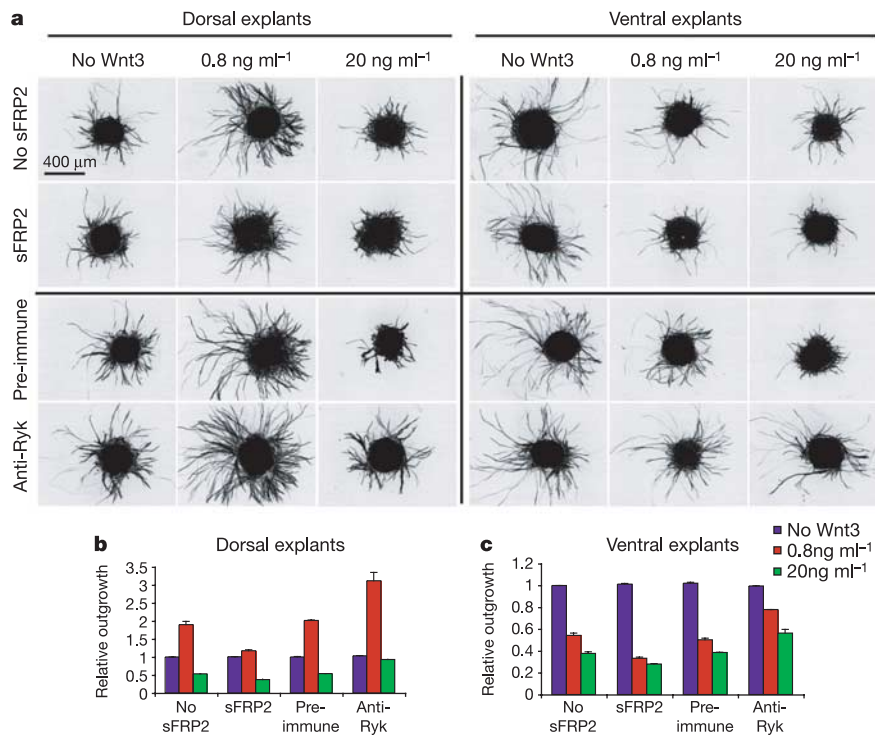


**Figure 3 | Wnt3 inhibits retinal ganglion cell axons via Ryk and stimulates retinal ganglion cell axons via Frizzled(s).** **a**, Chick E6 retinal explants from both dorsal and ventral retina were cultured on cover slips coated with low or high concentrations of Wnt3 recombinant protein in the presence of preimmune or anti-Ryk antibodies or in the presence of sFRP2. Wnt3 inhibition of ventral explants at both concentrations and of dorsal explants

at high concentrations can be blocked by anti-Ryk antibodies but cannot be blocked by sFRP2. Stimulation to dorsal retinal explants at lower Wnt3 concentrations can be blocked by sFRP2 but cannot be blocked by anti-Ryk antibodies. **b**, **c**, Quantification of dorsal (**b**) and ventral (**c**) explants in the Ryk antibody blocking and sFRP2 blocking experiments at different Wnt3 concentrations. Scale bar in **a**, 400  $\mu$ m.

ventral axons contain an unknown repulsive Wnt3 guidance receptor other than Ryk.

To address whether Frizzled(s) mediate stimulation or inhibition by Wnt3, we tested the purified sFRP2 protein at two concentrations of Wnt3. The stimulation of dorsal explants at low concentrations of Wnt3 (0.8 ng ml<sup>-1</sup>) can be blocked by sFRP2 (0.2  $\mu$ g ml<sup>-1</sup>),

whereas the inhibition of ventral and dorsal axons at a higher Wnt3 concentration (20 ng ml<sup>-1</sup>) cannot be blocked by sFRP2 (Fig. 3a).

#### Ectopic Wnt3 expression in tectum repelled the termination zones

To test whether Wnt3 repels ventral axon termination zones *in vivo*,

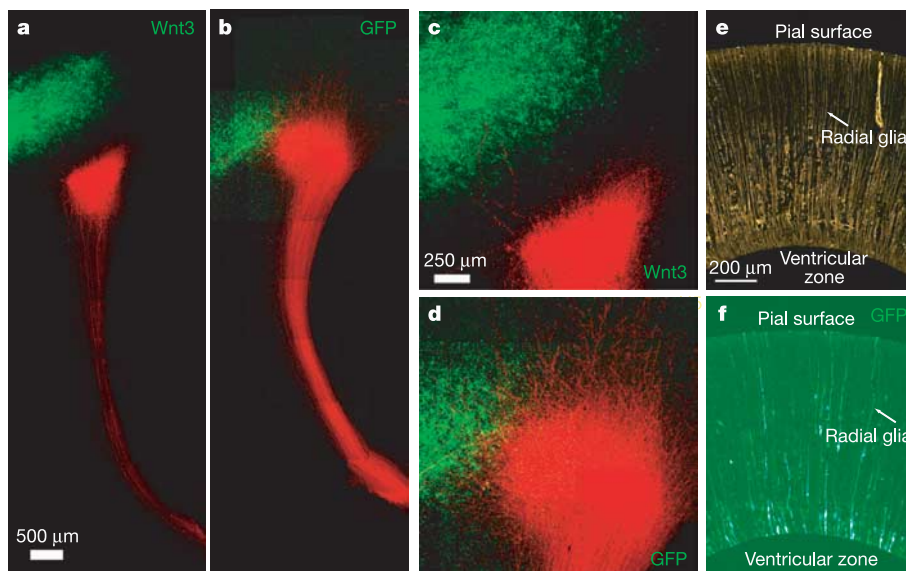


**Figure 4 | Termination zone of abnormalities in tectum ectopically expressing Wnt3.** **a**, RGC axon termination zones are repelled by Wnt3 expression (green area) ( $n = 7$ ). **b**, Normal termination zone formation of RGC axons in the tectal area expressing GFP control ( $n = 6$ ). **c**, Higher magnification of **a**. **d**, Higher magnification of **b**. **e**, Immunostaining of chick

E14 optic tectum with an antibody against a radial glial marker, H5, showing the presence of radial glial fibres. **f**, Immunostaining of chick E14 optic tectum electroporated with a GFP construct in the ventricular zone, showing that GFP protein was transported to the pial surface along the radial glial cells. Scale bars: **a**, **b**, 500  $\mu$ m; **c**, **d**, 250  $\mu$ m; **e**, **f**, 200  $\mu$ m.

we overexpressed Wnt3 by electroporation in the ventricular zone of chick optic tectum. Because the tectum is patterned by E3, expressing Wnt3 four days later (E7) should not alter the patterning of tectum<sup>21</sup>. In addition, we tested the expression pattern of ephrinB1 in the chick tectum electroporated with Wnt3 and found that the normal medial–lateral gradient of ephrinB1 was not altered (Supplementary Fig. 5b).

We electroporated a Wnt3 expression construct at E7, traced RGC axon termini with DiI injection at E13, and harvested tecta on E14 (Supplementary Fig. 5a). We found that the RGC axon termination zone, labelled with DiI, was repelled by ectopic Wnt3 (Fig. 4a, c,  $n = 7$ ) as compared to the green fluorescent protein (GFP) only (Fig. 4b, d,  $n = 6$ ), confirming a repulsive role of Wnt3 in guiding the termination of RGC axons. Immunostaining with the radial glial marker, H5, confirmed that radial glial fibres are present in chick tectum at this stage (Fig. 4e). We also stained a slice of chick optic tectum electroporated with a GFP construct in the ventricular zone with a GFP antibody, and found that many radial glial cells were expressing GFP. GFP was also detected all the way on the pial surface, confirming that proteins expressed in the radial glial cells in the ventricular zone introduced by electroporation can be transported to the pial surface (Fig. 4f).

### Dominant-negative Ryk caused a medial shift of the termination zone

Because Wnt3 is expressed in a medial-to-lateral decreasing gradient, we hypothesize that Wnt3 directs axons laterally to counteract EphrinB1, which promotes medially directed growth. Therefore, we predict that by blocking Wnt3–Ryk function, the termination zone should shift medially. Wnt3 knockout mice fail in early embryonic patterning and Wnt3 is also important for early nervous system development, making it impossible to examine the function of Wnt3 *in vivo* using the conventional knockout mouse approach<sup>22</sup>. Ryk knockout mice die at birth<sup>23</sup> and cannot be used to evaluate the function of Wnt3–Ryk in mice as termination zones form at postnatal day 8<sup>10</sup>. To circumvent this difficulty, we generated a dominant-negative form of Ryk and expressed it in chick RGCs in the dorsal aspect of retina by *in ovo* electroporation at E5 (Supplementary Fig. 6a, right panel). The truncated Ryk protein only contains Ryk ectodomain and the transmembrane domain, missing the intracellular domain. The intracellular domain was shown to be required for axon guidance in the fly homologue, *Derailed*<sup>15</sup>. It is unlikely that the expression of the truncated Ryk in the retina at E5 will affect dorsal–ventral fate mapping. First, the intracellular domain of Ryk is dispensable in cell fate determination, as a truncated Ryk, including only the extracellular and the transmembrane domains, can rescue cell fate phenotypes in *Caenorhabditis elegans*<sup>24</sup>. Second, chick retinal cell fate is determined at an earlier stage (Hamilton–Hamburger stage 10 or E1.5), and after stage 10, fate is already determined, as suggested by reported studies<sup>21</sup>. For example, cells from the anterior eye anlage were manipulated to form the posterior anlage, and they maintained the anterior identity and selected a tectal target consistent with the anterior origin<sup>21</sup>. Third, we examined the expression patterns of cell differentiation markers, such as EphrinB1 and EphB2, and found that their normal graded expression patterns were not affected (Supplementary Fig. 6b).

To visualize RGC axons, we co-electroporated a mixture of the dominant-negative Ryk and a cytomegalovirus (CMV)–GFP construct at a 3:1 ratio (Ryk DN:GFP). Mixing these two constructs allows us to determine the width of the termination zone (because some of the RGC axons will express the GFP control only) and the relative medial–lateral position of the termination zone when the Ryk dominant-negative construct is expressed. We elected to express the Ryk dominant-negative construct in the dorsal retina because Ryk is expressed at lower levels there and, therefore, it may be easier to block the endogenous Ryk function by the truncated Ryk. In addition, the

dorsal axons normally target the lateral optic tectum, so we can test the hypothesis that a Wnt–Ryk interaction mediates lateral-directed axon termination.

We found that RGC axons, co-electroporated with the dominant-negative Ryk construct, formed wide termination zones that extended more medially (Fig. 5b) compared to GFP control (Fig. 5a). These termination zones typically expand to at least twice the normal size, and the medial extreme of the termination zone extended widely towards the dorsal midline and only shifted medially.

### Dominant-negative Ryk eliminated lateral-directed interstitial branches

To further characterize the topographic map shift and analyse interstitial branches, we created a construct with CMV-enhanced chick  $\beta$ -actin promoter driving dominant-negative Ryk followed by

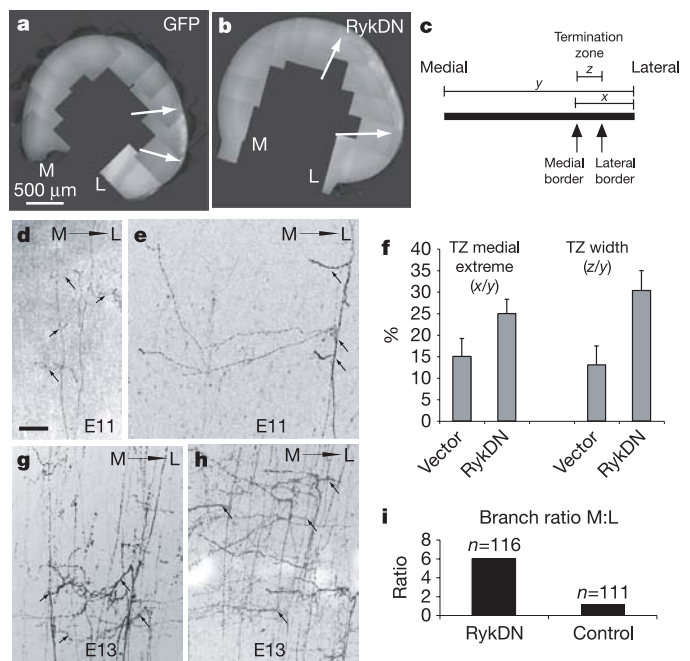


**Figure 5 | Ryk is required for normal medial–lateral patterning of RGC axon termination.** **a**, Normal termination zone of dorsal retinal ganglion cell axons in chick tectum visualized by eGFP in a control construct (CMV–eGFP) in 300  $\mu$ m vibratome sections perpendicular to the anterior–posterior axis of the tecta contralateral to retinas. eGFP was directly visualized by fluorescence. **b**, Much diffused termination zone (TZ) of dorsal RGC axons expressing a dominant-negative (DN) Ryk construct. The termination zone shifted medially. **c**, Diagram showing the quantification method. Dorsal RGC axons terminate at the lateral edge of the tectum. Termination zone ( $z$ ) is the area with eGFP signal observed in the vibratome section. The TZ width is defined as the ratio of the length of the termination zone ( $z$ ) over the entire length of the tectum along the medial–lateral axis ( $y$ ). The TZ medial extreme is defined as the ratio of the distance from the lateral edge to the medial border of the termination zone ( $x$ ) over the distance of the entire medial–lateral axis ( $y$ ). The termination zone shifted medially and expanded in size when dominant-negative Ryk was expressed in the dorsal retinal ganglion cells. **d, g**, Both medial- and lateral-directed interstitial branches were observed emerging from the primary RGC axons expressing a eGFP control ( $n$  of tecta = 20). Leftward arrows indicate medial-directed branches. Rightward arrows indicate lateral-directed branches. **e, h**, Interstitial branches of retinal ganglion cells in the tectum pointed medially from primary RGC axons expressing dominant-negative Ryk, visualized by an IRES–eGFP marker ( $n$  of tecta = 27). Virtually no lateral-directed interstitial branches were observed at the termination zone. **f**, Quantification of medial spread and width of termination zone. **i**, Quantification of ratio of medial- and lateral-directed interstitial branches in RGC axons expressing dominant-negative Ryk and a eGFP control.

internal ribosomal entry site (IRES)-eGFP. Using this construct, all green axons should express the dominant-negative Ryk, allowing us to observe details of branch formation from the primary RGC axon shafts. This construct was introduced into RGC cells at E7 by electroporation, and the axon projections in the whole mount tectum were analysed from E11 to E13 (Fig. 5d–h). We found that in Ryk dominant negative-expressing axons, very few lateral-directed branches were observed at the termination zone and only medial-directed branches were present (Fig. 5e, h) and they were typically longer than in GFP control-electroporated axons, which displayed almost equal length and frequency of interstitial branches of both directions (Fig. 5d, g). These long medial branches eventually formed multiple smaller termination zones medial to their appropriate positions along the medial–lateral axis of the tectum (not shown).

## Discussion

Our study proposes that Wnt3 acts as a lateral mapping force in the optic tectum to counterbalance the EphrinB1–EphB interaction, which is a medial-directed mapping force<sup>10</sup> (Fig. 6a). The Wnt3 and EphrinB1 signalling pathways are probably independent of each other, as blocking of Wnt–Ryk function allows axons to still respond to the EphrinB1–EphB function, causing termination zones to shift medially (Fig. 6b), and the termination zones to shift laterally in EphB2/B3 double knockout mice (Fig. 6c)<sup>10</sup>. However, one cannot exclude the possibility that these two signalling pathways may modulate each other's activity in the same growth cone. *Wnt3* is the only *Wnt* gene that displays a continuous medial–lateral graded expression in the ventricular zone of the tectum and superior colliculus. Initial mapping of the retinal axons occurs at the pial surface, which contains molecular cues such as the EphrinAs and EphrinB1 that are synthesized by radial glial cells and transported along the radial glia to the pial surface. However, our current study cannot exclude the possible roles of other Wnts, which might contribute to map formation through diffusion from other layers of the tectum or superior colliculus. Owing to technical limitations of *in ovo* electroporation, it is not feasible to systematically examine

map formation throughout the entire medial–lateral axis to confirm that these two mapping forces function uniformly, or to determine whether there are additional mapping forces. More sophisticated genetic manipulations will be needed to address these questions.

The graded and biphasic activity of Wnt3 in different dorsal–ventral retinal axons is reminiscent of EphrinAs along the anterior–posterior axis<sup>25</sup>. The differential responsiveness to EphrinAs was proposed to be caused by repulsion versus adhesion, as repulsion requires cleaved EphrinAs and adhesion requires glycosylphosphatidylinositol (GPI)-linked ephrinAs<sup>25</sup>. Our study suggests an alternative model such that a repulsive Wnt–Ryk pathway competes with an attractive Wnt–Frizzled interaction to titrate the response to Wnt3 protein at different concentrations. The graded response may be determined by the gradient of Ryk expression in the dorsal–ventral axis. Ventral RGCs express more Ryk, whereas dorsal RGCs have less Ryk. Expression of *frizzled5* appears to be even along the dorsal–ventral axis. The net outcome of this competition is varied in a graded fashion in growth cones along the dorsal–ventral axis, and thus determines the topographic connections.

Neurons typically connect to multiple targets and even different brain centres. Multiple forms of axon branches are observed, including collateral and interstitial branches. During retinotectal topographic mapping, RGCs project interstitial branches. These interstitial branches extend medially or laterally towards their future termination zone<sup>26</sup>. Once interstitial branches reach their termination zone, they form elaborate termini and the axons that have overshot are pruned back (in chick and mice). Therefore, the initial direction and growth of interstitial branches influence the position of the termination zone. We found that the Wnt–Ryk pathway is required for the laterally directed interstitial branches *in vivo*. Blocking Ryk by a truncated Ryk receptor eliminated nearly all laterally directed branches, leaving only the medially directed branches, which are unusually long. In contrast, in EphB2 and EphB3 double knockout mice, interstitial branches were found preferentially directed laterally<sup>10</sup>. Therefore, Wnt3 and EphrinB1 are opposing guidance activities for regulating interstitial branches in medial–lateral retinotectal mapping (Fig. 6).

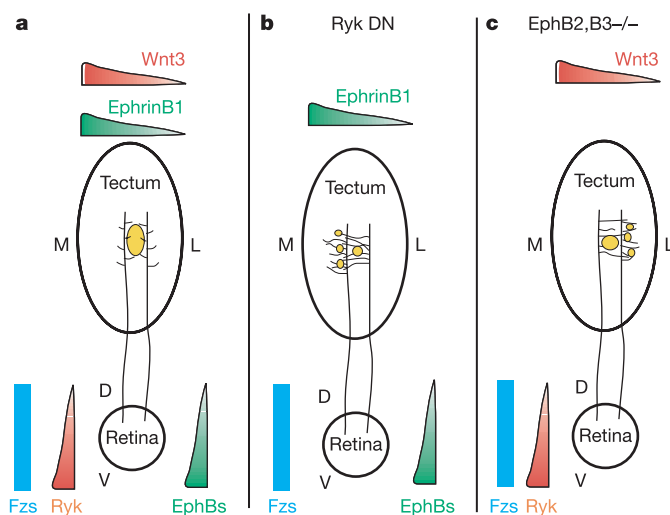


**Figure 6 | Model of two counterbalancing forces for medial–lateral map formation.** **a**, Wnt3 is a lateral mapping force, which is mediated by Ryk and Frizzled. Ventral axons are repelled by Wnt3, but dorsal axons are attracted by low Wnt3 and repelled by high Wnt3. Although the effect is biphasic along the dorsal–ventral axis of retina, the overall function of Wnt signalling is to drive interstitial branches laterally. The medial mapping force is EphrinB1 read by EphB2 and B3 via an attractive mechanism. **b**, When Wnt3 repulsion is blocked by a Ryk dominant-negative construct, EphrinB1–EphBs signalling causes interstitial branches to project medially only, causing a medial shift of the map. **c**, When EphrinB1–EphBs signalling was eliminated, interstitial branches project laterally, as shown in ref. 10.

## METHODS

**Retinal explant cultures.** Retinal explant cultures were performed according to a modified procedure from a previously described method<sup>25</sup>. For details, see Supplementary Methods.

***In ovo* electroporation.** For Wnt3 ectopic overexpression, E7 chick tecta were electroporated with a CMV-Wnt3 expression construct mixed with a CMV-enhanced GFP (eGFP) construct (Wnt3:eGFP = 3:1) to visualize the electroporated area, and at E13 RGC axons were labelled with a focal injection of Di-I (diagram in Supplementary Fig. 5a). Tecta were then harvested at E14 for analyses of retinotectal projections (Fig. 4).

To characterize the termination zone of RGC axons, E5 chick retinas were electroporated in dorsal retina with a Ryk dominant-negative construct mixed with eGFP construct (3:1 ratio) (Supplementary Fig. 6a). On E14, contralateral tecta were harvested, and sectioned (250–300  $\mu$ m thick) perpendicular to the anterior–posterior axis with a vibratome. Sections were photographed on an epifluorescence microscope (Fig. 5a, b). Results were quantified from four Ryk dominant-negative and three control experiments (Fig. 5c, f). The relative medial–lateral positions of termination zones are dependent on the dorsal–ventral position of electroporation in the retina. Therefore, the results of the medial extreme (the most medial border) of the termination zone have higher system error. However, the results on the width of termination zones are independent of the dorsal–ventral positions of electroporation and therefore are less prone to variations caused by the site of electroporation.

For analyses of interstitial branches, E7 chick retinas were electroporated with pCIG Ryk dominant-negative IRES GFP and contralateral tecta were harvested from E11 to E13 (Supplementary Fig. 6a). Tecta were flat mounted on glass slides and photographed with a confocal microscope (Fig. 5d, e, g, h). Results were quantified by counting 116 branches in 27 tecta for the Ryk dominant-negative construct and 111 branches in 20 tecta for the GFP only control (Fig. 5i).

**Cloning and constructs.** Detailed cloning and construct information can be found in Supplementary Methods.

**In situ hybridization, immunohistochemistry and western blot.** *In situ* hybridization and immunohistochemistry were performed as previously described<sup>11</sup>. For quantification of *in situ* signal density, digital images of *in situ* hybridizations were taken and resized to 600 × 450 pixels. The positive greyscale signals along the dorsal–ventral axis of the RGC layer of retina or the medial–lateral extent in the ventricular zone of the chick optic tectum and mouse superior colliculus were quantified with NIH Image by plot profile. The average signal density of each segment, retinal RGC layer or the ventricular zone of tectum or superior colliculus was divided into six equal segments and calculated. Data from five sections were collected and averaged. Graphs were created using GraphPad Prism after data were normalized by defining the largest value as 100%. Owing to the nonlinear nature of the enzyme reaction, this quantification represents the direction of the *in vivo* gradient but may not reflect the actual steepness.

Polyclonal anti-Wnt3 antibodies were purchased from Zymed Laboratories, Inc and used at 1 µg ml<sup>-1</sup> for western blot (1:100 dilution). H5 (1:100 dilution for immunohistochemistry) and E7 (1:500 dilution for immunohistochemistry) were monoclonal antibodies purchased from Developmental Biology Hybridoma Bank. Purified anti-Ryk antibodies were diluted 1:500 for immunostaining (Supplementary Fig. 3) and 1:1,000 for western blot (Supplementary Fig. 4e).

**Wnt receptor binding assays.** The protocol for binding assay was performed as previously published<sup>27,28</sup>. Details of methods can be found in Supplementary Methods.

Received 7 July; accepted 19 October 2005.

Published online 9 November 2005.

- Prestige, M. C. & Willshaw, D. J. On a role for competition in the formation of patterned neural connexions. *Proc. R. Soc. Lond. B* **190**, 77–98 (1975).
- Gierer, A. Model for the retino-tectal projection. *Proc. R. Soc. Lond. B* **218**, 77–93 (1983).
- Fraser, S. E. & Hunt, R. K. Retinotectal specificity: models and experiments in search of a mapping function. *Annu. Rev. Neurosci.* **3**, 319–352 (1980).
- Fraser, S. E. & Perkel, D. H. Competitive and positional cues in the patterning of nerve connections. *J. Neurobiol.* **21**, 51–72 (1990).
- Flanagan, J. G. & Vanderhaeghen, P. The ephrins and Eph receptors in neural development. *Annu. Rev. Neurosci.* **21**, 309–345 (1998).
- Frisen, J. *et al.* Ephrin-A5 (AL-1/RAGS) is essential for proper retinal axon guidance and topographic mapping in the mammalian visual system. *Neuron* **20**, 235–243 (1998).
- Feldheim, D. A. *et al.* Topographic guidance labels in a sensory projection to the forebrain. *Neuron* **21**, 1303–1313 (1998).
- Feldheim, D. A. *et al.* Genetic analysis of ephrin-A2 and ephrin-A5 shows their requirement in multiple aspects of retinocollicular mapping. *Neuron* **25**, 563–574 (2000).
- Mann, F., Ray, S., Harris, W. & Holt, C. Topographic mapping in dorsoventral axis of the *Xenopus* retinotectal system depends on signalling through ephrin-B ligands. *Neuron* **35**, 461–473 (2002).
- Hindges, R., McLaughlin, T., Genoud, N., Henkemeyer, M. & O'Leary, D. D. EphB forward signalling controls directional branch extension and arborization required for dorsal–ventral retinotopic mapping. *Neuron* **35**, 475–487 (2002).
- Lyuksyutova, A. I. *et al.* Anterior–posterior guidance of commissural axons by Wnt-frizzled signalling. *Science* **302**, 1984–1988 (2003).
- Drescher, U. *et al.* *In vitro* guidance of retinal ganglion cell axons by RAGS, a 25 kDa tectal protein related to ligands for Eph receptor tyrosine kinases. *Cell* **82**, 359–370 (1995).
- Smolich, B. D., McMahon, J. A., McMahon, A. P. & Papkoff, J. Wnt family proteins are secreted and associated with the cell surface. *Mol. Biol. Cell* **4**, 1267–1275 (1993).
- Willert, K. *et al.* Wnt proteins are lipid-modified and can act as stem cell growth factors. *Nature* **423**, 448–452 (2003).
- Yoshikawa, S., McKinnon, R. D., Kokel, M. & Thomas, J. B. Wnt-mediated axon guidance via the *Drosophila* Derailed receptor. *Nature* **422**, 583–588 (2003).
- Liu, Y. *et al.* Ryk-mediated Wnt repulsion regulates posterior-directed growth of corticospinal tract. *Nature Neurosci.* **8**, 1151–1159 (2005).
- Hovens, C. M. *et al.* RYK, a receptor tyrosine kinase-related molecule with unusual kinase domain motifs. *Proc. Natl Acad. Sci. USA* **89**, 11818–11822 (1992).
- Dann, C. E. *et al.* Insights into Wnt binding and signalling from the structures of two Frizzled cysteine-rich domains. *Nature* **412**, 86–90 (2001).
- Hsieh, J. C., Rattner, A., Smallwood, P. M. & Nathans, J. Biochemical characterization of Wnt-frizzled interactions using a soluble, biologically active vertebrate Wnt protein. *Proc. Natl Acad. Sci. USA* **96**, 3546–3551 (1999).
- Patthy, L. The WIF module. *Trends Biochem. Sci.* **25**, 12–13 (2000).
- Mey, J. & Thanos, S. Development of the visual system of the chick. I. Cell differentiation and histogenesis. *Brain Res. Rev.* **32**, 343–379 (2000).
- Liu, P. *et al.* Requirement for Wnt3 in vertebrate axis formation. *Nature Genet.* **22**, 361–365 (1999).
- Halford, M. M. *et al.* Ryk-deficient mice exhibit craniofacial defects associated with perturbed Eph receptor crosstalk. *Nature Genet.* **25**, 414–418 (2000).
- Inoue, T. *et al.* *C. elegans* LIN-18 is a Ryk ortholog and functions in parallel to LIN-17/Frizzled in Wnt signalling. *Cell* **118**, 795–806 (2004).
- Hansen, M. J., Dallal, G. E. & Flanagan, J. G. Retinal axon response to ephrin-as shows a graded, concentration-dependent transition from growth promotion to inhibition. *Neuron* **42**, 717–730 (2004).
- McLaughlin, T., Hindges, R. & O'Leary, D. D. Regulation of axial patterning of the retina and its topographic mapping in the brain. *Curr. Opin. Neurobiol.* **13**, 57–69 (2003).
- Flanagan, J. G. & Leder, P. The kit ligand: a cell surface molecule altered in steel mutant fibroblasts. *Cell* **63**, 185–194 (1990).
- Cheng, H. J. & Flanagan, J. G. Identification and cloning of ELF-1, a developmentally expressed ligand for the Mek4 and Sek receptor tyrosine kinases. *Cell* **79**, 157–168 (1994).

**Supplementary Information** is linked to the online version of the paper at [www.nature.com/nature](http://www.nature.com/nature).

**Acknowledgements** This work was supported by the Alfred Sloan Foundation, the Scheweppe Foundation and NINDS. We thank F. Polleux for the pCIG2 vector (CMV-enhanced β-actin promoter with IRES GFP marker) and A. G. Fenstermaker for critical reading of the manuscript.

**Author Information** Reprints and permissions information is available at [npg.nature.com/reprintsandpermissions](http://npg.nature.com/reprintsandpermissions). The authors declare no competing financial interests. Correspondence and requests for materials should be addressed to Y.Z. ([yzou@bsd.uchicago.edu](mailto:yzou@bsd.uchicago.edu)).